

Modeling of Interior Permanent Magnet Synchronous Motor using Transient Simulation Techniques

Parvathi M. S¹ and Dr Nisha G. K²

¹ PG Student, Dept of EEE, Mar Baselios College of Engineering and Technology, Trivandrum, Kerala, India

²Associate Professor, Dept of EEE, Mar Baselios College of Engineering and Technology, Trivandrum, Kerala, India

Abstract

This paper presents a detailed modeling of the Interior Permanent Magnet Synchronous Motor (IPMSM) drive system. The modeling is done with the aid of Transient Simulation techniques and the equations are obtained in the Forward Euler form. It also discusses the main differences between the two types of PMSMs. The dynamic modeling of IPMSM is done in the synchronous reference frame and the corresponding speed waveform for a six pole machine is obtained.

Keywords: Interior Permanent Magnet Synchronous Motor (IPMSM), Transient Simulation Technique and Synchronous Reference Frame.

1. Introduction

Permanent magnets have not been used for electrical machines for a long time because the development of the permanent magnet materials was not mature until mid-20th century. After the invention of Alnico, Ferrite, Nd-Fe-B (Neodymium-Iron-Boron), Sm-Co (Samarium-Cobalt) materials, permanent magnets were widely used for DC machines in small power applications, such as automobile auxiliary motors. Recently, the improvement of the quality of permanent magnet materials and the technical advances of the control methods allow replacing induction machines with permanent magnet machines in many industrial areas. Nowadays, with the rapid development of electric power electronics and rare earth permanent magnetic materials, increasingly sophisticated research is made in Permanent magnet motor [1]. The use of permanent magnet has replaced the need of slip rings for field excitation which results in low maintenance and low losses in the rotor [2]. Owing to its other remarkable characteristics of strong coupling, nonlinearity and multivariable nature, application of Permanent Magnet Synchronous Motors (PMSMs) are increasingly found in areas such as national defence, agriculture, robotics, aerospace technology and daily life. In [3], a DQ model of PMSM has explained and two different approaches of modeling PMSMs in a real time digital simulator were proposed.

This paper analyses the modeling of interior type PMSM using the various Transient simulation technique. The interior PMSM is to be modeled in synchronous reference frame and the various voltage and torque equations are formed.

2. Permanent Magnet Synchronous Motor

2.1. Conventional PMSM

Permanent Magnets (PMs) eliminate the use of field exciting coils and slip rings for current conduction. Due to the absence of field winding inside the rotor, PM motors have low inertia. The field strength is so high that the motor volume can be reduced [4]. Further, since there is no copper loss on the secondary winding, the PM motors have higher efficiency than induction motors. Also, PMSMs are advantageous in incorporating the reluctance torque, in the field weakening range, so that they can be designed to have a wide constant power speed range (CPSR). As a result, PMSMs have higher power densities than any other type of motors.

As the greenhouse effect become a serious concern, the efficiency of home appliances become more important than ever. Due to recent reduction in PM material cost and growing concern for greenhouse gases, PMSMs are widely used in home appliances such as refrigerators, air conditioners, vacuum cleaners, washers etc. Also, hydraulic actuators in vehicles and aeroplanes are being replaced by PMSMs for higher fuel efficiency. Furthermore, PMSMs are popularly used as propulsion motors for hybrid electric vehicles and ships. The key characteristics of PMSM include is that it has no sparks and hence safer in explosive environments, faster, less noisy, more reliable and more efficient. It can run with or without position encoders and its more compact.

2.2. Types of PMSMs

The conventional PMSM can be classified into surface mounted PMSMs (SPMSM) and interior PMSMs (IPMSM). The difference lies in the location of PMs. When the PMs are mounted on the surface of the rotor, it's called SPMSM and if the PMs are buried inside the cavities of the rotor core, it's called IPMSM. A common problem in SPMSM lies in the methods of fixing PMs on the rotor surface. Glues are widely used, but they have aging effects under the stress of heat cycles and large centrifugal force [5]. If stainless band is used for fixing and protecting PMs, then loss will take place on the surface of the stainless steel due to the eddy current caused by slot harmonics and inverter PWM carrier. Further, the protecting devices like glass fibre or stainless steel require a larger air gap.

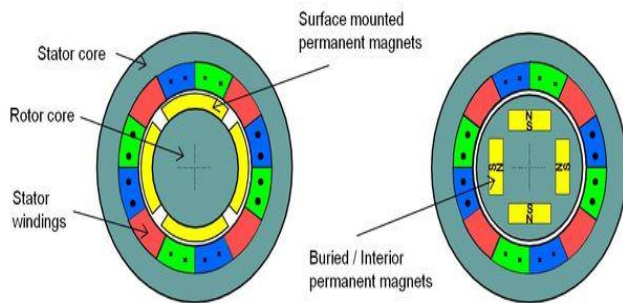


Fig. 1 Structure of Surface mounted PMSM and Interior PMSM

In IPMSMs, no fixation device is required since the PMs are inserted in the cavities. Further, PMs are protected from the stator MMF harmonics and slot harmonics, allowing for use of cost effective rectangular shaped magnets. The saliency ratio is unity for SPMSM but greater than unity in the case of IPMSM. Also, the IPMSM has high power density when compared to the SPMSM.

3. Interior PMSM

In addition to the merit of high-speed operation, the useful properties of IPMSM includes field weakening capability with high inductance, under-excited operation for most load conditions, reducing the risk of demagnetization of permanent magnets, increase the resistance against mechanical impacts and corrosion and high temperature capability [6]. The relative recoil permeability of certain magnetic materials used for permanent magnets are Ferrite: 1.05 ~ 1.15, Nd-Fe-B: 1.04 ~ 1.11 and Sm-Co: 1.02 ~ 1.07. From these permeability values, we can understand that the permeabilities are close to one although they can retain high residual field density. From the magnetic reluctance view point, they can be treated the same as

vacuum. Since the permeability of widely used PMs are close to unity, the PMs look like air in the view of magnetic reluctance. Therefore, the reluctance profile changes depending on whether the PMs are set on the rotor surface or in the cavities of the rotor [7]. The reluctance variation is reflected in the difference of d and q axis inductance values.

The reluctances are different depending on the flux paths in IPMSMs. The Figure 2 shows the d-axis and q-axis flux paths of IPMSM. According to the figure, PMs are encountered following the d-axis flux, whereas no PM is found in the q-axis. Hence, the d-axis reluctance is greater than that of the q-axis, i.e, the d-axis inductance is smaller than that of the q-axis.

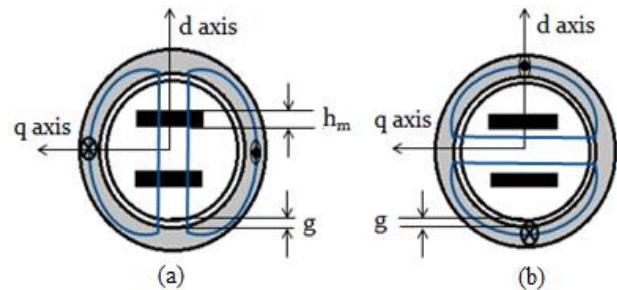


Fig. 2 Flux paths of IPMSM: (a) d-axis flux path, (b) q-axis flux path

Specifically we obtain the inductance values as in the equation (1) and (2).

$$L_d = \frac{\mu_0 N^2 A}{2(g + h_m)} \quad (1)$$

$$L_q = \frac{\mu_0 N^2 A}{2g} \quad (2)$$

where L_d and L_q represents the d-axis and q-axis inductances, μ_0 represents the relative permeability value, N gives the number of turns of the d-axis winding, A is the air gap area through which the flux crosses, g is the air gap and h_m gives the width of the PM used. Thus, $L_d < L_q$ for an IPMSM. This inductance asymmetry generates the reluctance torque, and the reluctance torque contributes to increasing the shaft torque with negative d-axis current.

4. Dynamics in Synchronous Reference Frame

In IPMSM, the inductance changes depending on the rotor position. The flux linkage change is described by a sinusoidal function of the rotor angle (θ). Considering the flux linkage of a-phase winding for different rotor

positions, we can note that the effective air gap changes, as the rotor rotates.

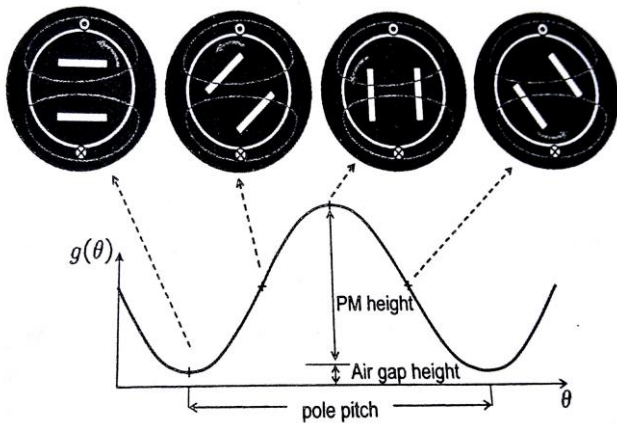


Fig. 3 Effective air gap as a function of rotor angle

The effective air gap reaches its peak, when the flux lines cross the cavities at the right angle [8], [9]. However, it reduces to the minimum value, when the lines do not cross the cavities. The final voltage equation of IPMSM dynamics in the synchronous reference frame can be given as in equation (3) and (4).

$$v_d^e = r_s i_d^e + L_d \frac{d}{dt} i_d^e - \omega L_q i_q^e \quad (3)$$

$$v_q^e = r_s i_q^e + L_q \frac{d}{dt} i_q^e + \omega L_d i_d^e + \omega \varphi_m \quad (4)$$

From the equation (3) and (4), it can be noted that the coupling terms, $-\omega L_q i_q^e$ and $\omega L_d i_d^e$, are originated from rotating the coordinate and they make an interference between d and q dynamics.

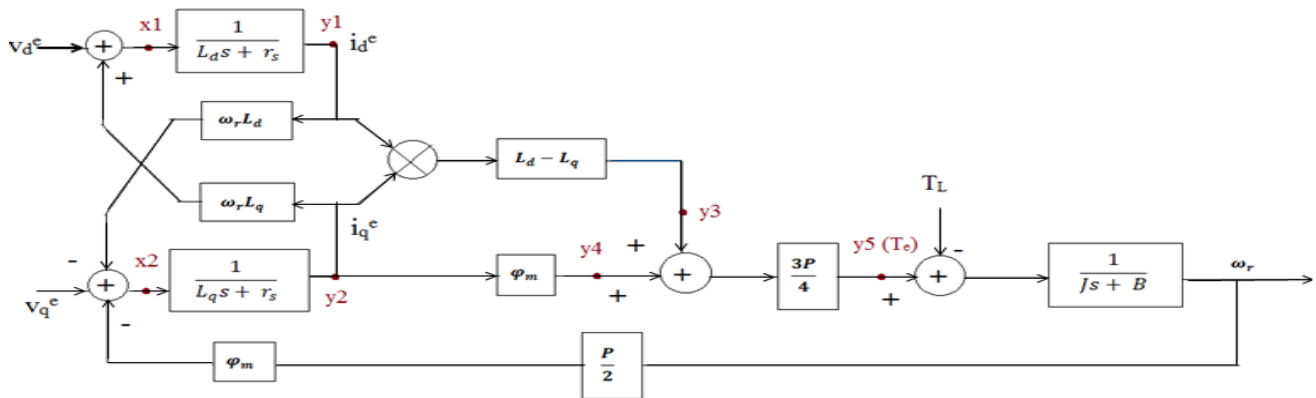
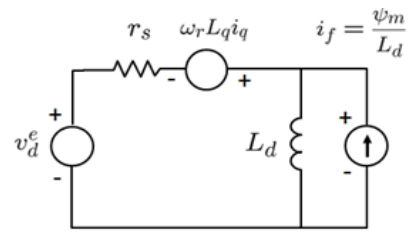


Fig. 5 Block diagram representing the IPMSM dynamics

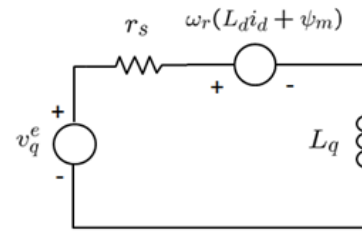
The rotor flux linkage is equivalently expressed as a product of d-axis inductance, L_d and a virtual current, i_f as depicted in the equation (5).

$$\varphi_m = L_d i_f \quad (5)$$

With i_f , a PMSM equivalent circuit can be depicted as shown in the Figure 4 (a) and (b).



(a)



(b)

Fig. 4 Equivalent circuit of IPMSM: (a) d-axis and (b) q-axis

5. IPMSM Dynamic Modeling

The Figure 5 shows a schematic block diagram for the modeling of PMSM. The block diagram contains 3 transfer functions $\frac{1}{L_d s + r_s}$, $\frac{1}{L_q s + r_s}$ and $\frac{1}{J s + B}$ which are to be solved using Transient Simulation Techniques.

The three methods for the Transient Analysis are (i) Forward Euler Method, (ii) Backward Euler Method and (iii) Trapezoidal Method. In the Forward Euler Method, the differential form of an element can be expressed as a function of its present and past values alone, unlike the Backward Euler Method which depends on the future values as well. The Trapezoidal Method can be explained as an average of the first and the second methods. The choice of method is depends on three major concerns, namely, accuracy, stability and the computational time [10]. The computational time required for Forward Euler Method is very less compared to the other two techniques, as it depends only on the past values and the so formed linear equations can be solved easily.

The modeling equations at the various nodes mentioned in the block diagram can be expressed in the equations from (6) to (13).

$$x_1^{n+1} = v_d^{\varepsilon n+1} + \omega_r L_q i_q^{\varepsilon n+1} \quad (6)$$

$$x_2^{n+1} = v_q^{\varepsilon n+1} - \omega_r L_d i_d^{\varepsilon n+1} - \omega_r^{n+1} \frac{P}{2} \varphi_m \quad (7)$$

The modeling equation for the d-axis and q-axis current in the synchronous reference frame can be expressed as in the equation (8) and (9).

$$y_1^{n+1} = i_d^{\varepsilon n+1} = \frac{h}{L_d} x_1^n + \left[\frac{L_d - R_s h}{L_d} \right] i_d^{\varepsilon n} \quad (8)$$

$$y_2^{n+1} = i_q^{\varepsilon n+1} = \frac{h}{L_q} x_2^n + \left[\frac{L_q - R_s h}{L_q} \right] i_q^{\varepsilon n} \quad (9)$$

$$y_3^{n+1} = (L_d - L_q) i_q^{\varepsilon n+1} i_d^{\varepsilon n+1} \quad (10)$$

$$y_4^{n+1} = \varphi_m i_q^{\varepsilon n+1} \quad (11)$$

The electromagnetic torque equation at the node y5 can be expressed as in equation (12).

$$T_s^{n+1} = \frac{3P}{4} \left((L_d - L_q) i_q^{\varepsilon n+1} i_d^{\varepsilon n+1} + \varphi_m i_q^{\varepsilon n+1} \right) \quad (12)$$

We can understand from the equation (12) that $\varphi_m i_q^{\varepsilon}$ is the electromagnetic torque based on Lorentz force, whereas $-(L_d - L_q) i_d^{\varepsilon} i_q^{\varepsilon}$ is the reluctance torque caused by the $(L_d - L_q)$ asymmetry.

The modeling equation for speed can be expressed as in equation (13).

$$\omega_r^{n+1} = \frac{h}{J} (T_s^{n+1} - T_l^{n+1}) + \frac{J - Bh}{J} \omega_r^n \quad (13)$$

6. Results and Simulations

According to the proposed method for the modeling of IPMSM using Transient Simulation Technique, run in SEQUEL (A Solver for circuit Equations with User-defined Elements), the motor parameters used are as in Table I.

Table 1. Motor Specifications

PARAMETERS	SPECIFICATIONS
Motor Power	20 kW
Rated speed	1000 rpm
Rated torque	190.98 Nm
Rated current	296 A
Rated voltage	176 V
Number of poles	6
L_d	0.395 mH
L_q	0.695 mH
r_s	6.5 mΩ
Flux(φ_m)	0.080 Wb
Inertia(J)	0.1 kgm ²
Damping Coefficient(B)	0

For no load condition, the rated speed of 1000 rpm is obtained and the waveform is as in Figure 6. The Figure 7 shows the rotor position waveform.

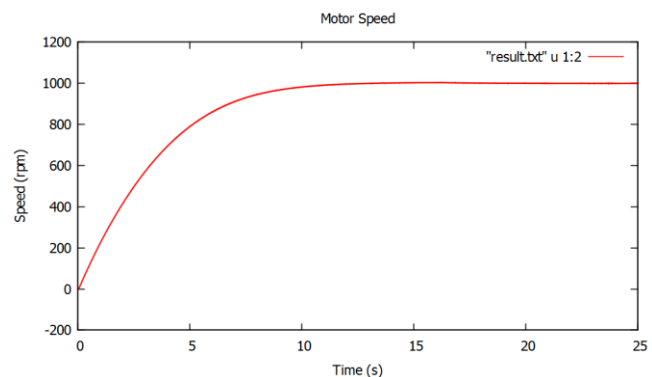


Fig. 6 Speed response under no load condition

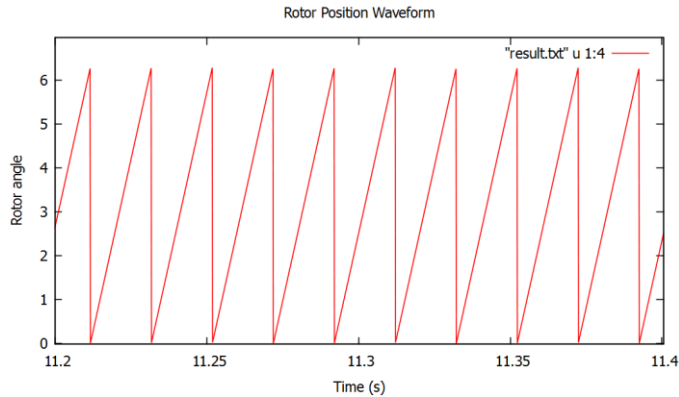


Fig. 7 Rotor position waveform of IPMSM

7. Conclusion

The dynamic modeling of and simulation study of IPMSM drive using Transient simulation technique is presented in this paper. A comparative study is made on the transient methods and the IPMSM is modeled using the Forward Euler method. The simulation results obtained indicate that the proposed mathematical modeling is effective.

References

- [1]. Zhonghui Zhang and Jiao Shu, "Matlab-based Permanent Magnet Synchronous Motor Vector Control Simulation," *Proceedings of the 3rd IEEE International Conference*, vol. 9, pp. 539-542, 2010.
- [2]. Jyoti Arawal and Sanjay Bodke, "Modeling and Simulation of a Torque Controlled Permanent Magnet Synchronous Motor Drive," *International Journal of Engineering Research & Technology (IJERT)*, vol. 3, issue 3, pp. 2098-2106, Mar. 2014.
- [3]. A. B. Dehkordi, A. M. Gole, T. L. Maguire, "Permanent Magnet Synchronous Machine Model for Real-Time Simulation," *International Conference on Power Systems Transients (IPST'05)*, June. 2005.
- [4]. Wencong Tu, Guangzhao Luo, Shengpan Ma and Xueli Fang, "Design of Permanent Magnet Synchronous Motor Real-Time Simulation Control System," *Proceeding of the IEEE International Conference on Information and Automation*, pp. 1124-1129, Aug. 2013.
- [5]. Parvathi M. S and Nisha G. K., "State of Art of PMSM Speed Control Using DTC and FOC Techniques," *International Journal of Advanced Research in Electrical, Electronics and Instrumentation Engineering (IJAREEIE)*, vol. 5, issue 6, Jun 2016.
- [6]. Lee, Seong Taek, "Development and Analysis of Interior Permanent Magnet Synchronous Motor with Field Excitation Structure," PhD diss., University of Tennessee, 2009.

- [7]. Kwang Hee Nam, "AC Motor Control and Electrical Vehicle Applications", CRC Press, 2010.
- [8]. P. C. Krause, O. Wasynczuk and S. D. Sudhoff, "Analysis of Electric Machinery, IEEE Press, 1995.
- [9]. D. W. Novotny and T. A. Lipo, "Vector Control and Dynamics of AC Drives, Clarendon Press, Oxford 1996.
- [10]. M. B. Patil, V. Ramanarayanan, and V. T. Ranganathan, "Simulation of Power Electronic Circuits", Narosa Publishing House Pvt. Ltd., New Delhi, 2013.

Biographies



Parvathi M. S was born in Trivandrum, India on 20th June 1990. She received B-Tech degree in Electrical and Electronics Engineering from Mohandas College of Engineering and Technology, Thiruvananthapuram, India in 2012 and is currently pursuing M-tech degree from Mar Baselios College of

Engineering and Technology, Thiruvananthapuram, India. Her area of interests includes Power Converters and Electrical Machines & Drives.



Nisha G.K. was born in Trivandrum, India on 20th May 1976. She received the B-Tech degree in Electrical and Electronics Engineering from TKM College of Engineering (University of Kerala) and M-Tech degree in Electrical Machines from Government College of Engineering, Trivandrum

(University of Kerala), Kerala, and Ph.D in Electrical Engineering from Government College of Engineering (University of Kerala) Trivandrum, India in 1997, 2000 and 2015 respectively. She has 15 publications in international journals and 8 international conferences at her credit. From 2001 onwards she was with the University College of Engineering, Trivandrum as Lecturer and with the Mar Baselios College of Engineering and Technology, Trivandrum as Associate Professor in the Department of Electrical Engineering. Her research interest includes ac drives, pulse width modulation and field oriented control. Ms. Nisha received Certificate of Merit (student) Award for the 2012 IAENG International Conference on Electrical Engineering held at Hong Kong and Best Paper Award at the 2013 Conference on Advance Engineering and Technology held at Mysore, India.